Complex spatial and temporally defined myelin and axonal degeneration in Huntington disease

H.D. Rosas[a,b,c,d,*], P. Wilkens[a,b,c], D.H. Salat[b,c,d,g], N.D. Mercaldo[d,1], M. Vangel[c,d,e,1], A.Y. Yendiki[c,d,f], S.M. Hersch[a]

[a] Department of Neurology, Massachusetts General Hospital, Harvard Medical School, Boston, MA, USA
[b] Center for Neuro-imaging of Aging and Neurodegenerative Diseases, Massachusetts General Hospital, Harvard Medical School, Boston, MA, USA
[c] Athinoula A. Martinos Center for Biomedical Imaging, Massachusetts General Hospital, Harvard Medical School, Boston, MA, USA
[d] Department of Radiology, Massachusetts General Hospital, Harvard Medical School, Boston, MA, USA
[e] Department of Biostatistics, Massachusetts General Hospital, Boston, MA, USA
[f] Harvard-MIT Division of Health Sciences and Technology, Cambridge, MA, USA
[g] Neuroimaging Research for Veterans Center, VA Boston Healthcare System, Boston, MA, USA

ARTICLE INFO

ABSTRACT

Although much prior work has focused on the basal ganglia and cortical pathology that defines Huntington's disease (HD), recent studies have also begun to characterize cerebral white matter damage (Rosas et al., 2006; Dumas et al., 2012; Poudel et al., 2014). In this study, we investigated differences in the large fascicular bundles of the cerebral white matter of gene-positive HD carriers, including pre-manifest individuals and early symptomatic patients, using recently developed diffusion tractography procedures. We examined eighteen major fiber bundles in 37 patients with early HD (average age 55.2 ± 11.5, 14 male, 23 female), 31 gene-positive, motor negative pre-symptomatic HD (PHD) (average age 48.1 ± 11.5, 13 male, 18 female), and 38 healthy age-matched controls (average age 55.7 ± 8.6, 14 male, 24 female), using the TRActs Constrained by UnderLying Anatomy (TRACULA) procedure available as part of the FreeSurfer image processing software package. We calculated the mean fractional anisotropy (FA) and the mean radial (RD) and axial diffusivities (AD) for each fiber bundle. We also evaluated the relationships between diffusion measures, cognition and regional cortical thinning. We found that early changes in RD of select tracts in PHD subjects were associated with impaired performance on neuropsychological tests, suggesting that early changes in myelin might underlie early cognitive dysfunction. Finally, we found that increases in AD of select tracts were associated with regionally select cortical thinning of areas known to atrophy in HD, including the sensorimotor, supramarginal and fusiform gyrus, suggesting that AD may be reflecting pyramidal cell degeneration in HD. Together, these results suggest that white matter microstructural changes in HD reflect a complex, clinically relevant and dynamic process.

1. Introduction

Huntington's disease is an autosomal dominantly inherited neurodegenerative disorder that is associated with progressive motor, psychiatric, and cognitive disability. Although considerable work has focused on the devastation of the basal ganglia and of select cortical regions in HD, including sensorimotor cortical areas, precuneus, portions of occipital, and superior temporal (Rosas et al., 2008b), white matter (WM) pathology has only recently been recognized as significant (Rosas et al., 2006; Poudel et al., 2014). Several studies have shown that mutant huntingtin expression is high in cerebral white matter

(Sapp et al., 1999) and aggregates have been found in axons undergoing degeneration, even in the absence of neuronal death (Yu et al., 2003), suggesting a potentially important role of white matter degeneration in clinical symptoms.

Diffusion Weighted Imaging (DWI) is a powerful technique to infer local fiber orientation of fiber bundles, which allows the reconstruction the major pathways in the brain. It also enables the measurement of several microstructural properties of WM. Fractional anisotropy (FA) refers to the degree to which there is a preferential direction in the diffusion of water molecules and is particularly sensitive to the coherence, density, and myelination of white matter fiber tracts (Basser

and Pierpaoli, 1996; Barkovich et al., 1999; Song et al., 2003; Bartzokis et al., 2007). Fibers that are more highly myelinated or organized in similar orientations lead to higher FA than fibers that are less well-organized or less myelinated (Pierpaoli et al., 2001). Axial diffusivity (AD) measures the magnitude of water diffusion along the preferential direction of diffusion; increases in AD have been associated with axonal loss and have been reported in advance of changes in white matter volume or gray matter volume loss in other neuro-degenerative diseases (Pievani et al., 2010; Agosta et al., 2011). Radial diffusivity (RD) measures the magnitude of diffusion orthogonal to the preferential direction; increases in RD have been associated with defects in the integrity of myelin. Early increases in RD and AD have been reported prior to measurable changes in either white matter or gray matter volume loss in HD (Rosas et al., 2010; Bohanna et al., 2011; Delmaire et al., 2013). These studies have set the stage for evaluating fundamentally distinct pathologies of white matter in HD.

In this study, we used a diffusion tractography method for the automated reconstruction of eighteen major cerebral WM fiber bundles entitled TRActs Constrained by UnderLying Anatomy (TRACULA) (Yendiki et al., 2014). This method uses global probabilistic tractography with anatomical priors. Prior distributions on the neighboring anatomical structures of each pathway are derived from an atlas and combined with the FreeSurfer cortical parcellation and subcortical segmentation of the subject that is being analyzed to constrain the tractography solutions. This also allows the bundles to be reconstructed without the need for manual interaction. Furthermore, the only information used from the atlas is the relative position of the bundles and their surrounding anatomical structures, and not the exact coordinates of the bundles in a template space. Therefore, TRACULA extracts diffusion measures in each subject's native space, without requiring perfect alignment of the subject to a template space, as would be the case for voxel-based approaches, and therefore allows for the quantification of white matter differences between populations in much greater detail than is possible with a voxel-based or ROI-based approach.

We studied a cohort of 38 individuals with early symptomatic HD (HD), 31 gene-positive pre-manifest individuals (PHD) and 37 age and gender matched controls. We evaluated patterns of WM alterations that differed amongst groups. Given that myelination is known to correlate with cognition (Ishibashi et al., 2006), we also sought to determine the relationship between altered RD of distributed tracts and impaired performance on motor, attentional and executive functions, all known to be impaired early during the HD prodrome (Paulsen et al., 2017). Finally, we sought to determine if there were any relationship between altered AD and regional cortical atrophy, specifically in areas that have been shown to atrophy in HD, including, sensorimotor cortex, precuneus, frontal areas, and higher order visual cortical areas (Rosas et al., 2008a).

Our findings suggest distinct patterns of myelin and axonal degeneration in the spectrum of HD and provide further evidence for the importance of white matter pathology in the clinical expression of HD.

2. Materials and methods

2.1. Participants

Thirty-eight Huntington's Disease (HD) patients, 31 premanifest Huntington's Disease (PHD) patients and 37 healthy controls (HC) were recruited for this study. PHD subjects were further subdivided into PHD$_{far}$ and PHD$_{near}$, the latter category including individuals within ten years of expected onset (Langbehn et al., 2010); this was done to determine how early changes in diffusion measures might be present. Study protocols were approved by the Partners Institutional Review Board; the study was carried out in accordance with the Declaration of Helsinki after informed consent was obtained from study participants. There was no statistically significant difference in age across groups. Details of the cohort are given in Table 1. Four controls were taking

SSRI's. Twelve PHD subjects were taking SSRI's; five were on neuroleptics; three were taking nutritional supplements. Eighteen HD subjects were taking SSRI's; seven were on neuroleptics; five were taking nutritional supplements.

2.2. Experimental design

2.2.1. MRI acquisition

Imaging data was collected at MGH in a Siemens Trio 3-Tesla magnetic resonance imaging scanner equipped with a 12-channel head coil. A T1 weighted Multi-Echo MPRAGE was collected with the following parameters: Repetition time (TR): 2530.00 ms, Echo times (TE): 1.64 ms, 3.5 ms, 5.36 ms and 7.22 ms. Flip angle: 7.00°, Voxel Sizes 1.0 isotropic, image matrix size $256 \times 256 \times 176$, Field of View (FOV) 256×256 mm. A diffusion weighted scan was collected with the following parameters: TR/TE/Flip angle 7980 ms/83 ms/0°, 60 non-colinear directions, b = 700 s/mm^2, 64 slices, $128 \times 128 \times 64$ image matrix.

2.2.2. Automated anatomical segmentation

Automated cortical parcellations and subcortical segmentation were obtained through processing and reconstruction of the anatomical data using FreeSurfer (https://surfer.nmr.mgh.harvard.edu, software package version 5.3), as described previously (Rosas et al., 2011).

2.2.3. Tractography of 18 major WM tracts

Diffusion-weighted images were processed in a blinded fashion, using TRActs Constrained by UnderLying Anatomy (TRACULA), available as part of FreeSurfer (Yendiki et al., 2011; Yendiki et al., 2014). In order to reconstruct select WM bundles, TRACULA uses prior information of the anatomy from a set of training participants where the tracts of interest were labeled manually. This prior information is the probability of each tract to travel through or next to (in the left, right, anterior, posterior, etc. directions) each of the cortical and subcortical segmentation labels from FreeSurfer. The output of TRACULA is a probabilistic distribution for each of the 18 tracts, derived in the individual diffusion space rather than transformed from an average brain space (Yendiki et al., 2014).

Participant data was first preprocessed to correct for simple head motion and eddy currents by aligning the diffusion weighted images to an average of the first b = 0 image of the diffusion series, using a standard linear registration tool available as part of FSL (http://www.fmrib.ox.ac.uk/fsl). FreeSurfer's boundary-based registration method (Greve and Fischl, 2009) was used for the affine intra-subject alignment between the diffusion-weighted and anatomical images, and to an MNI152 template. Tensors were fit to the DWI data using a standard least squares tensor estimation method and FA, AD, and RD volumes were computed from the tensors. Note that tensors were used to compute these measures, and not for the tractography itself instead of the tensor model, TRACULA uses FSL's bedpostX tool to fit the ball-and-stick model of diffusion, comprising two anisotropic compartments per voxel; this models distinct axon populations and one isotropic compartment per voxel. TRACULA then uses the individual participant's local diffusion orientations, from the anisotropic compartments of the ball-and-stick model, as well as the participant's cortical and subcortical segmentation labels, combined with prior information on each tract's position relative to these labels based on the training set to estimate the probability distributions of each tract. This allows the reconstruction of volumetric distributions of major WM pathways included in the atlas and the extraction of tensor-based measures (FA, AD, and RD) for each of the reconstructed pathways. The major WM pathways include the forceps major (FM), forceps minor (Fm), L/R corticospinal tract (CST), L/R inferior longitudinal fasciculus (ILF), L/R uncinate fasciculus (UNC), L/R anterior thalamic radiation (ATR), L/R cingulum-cingulate gyrus bundle (CCG), L/R cingulum-angular bundle (CAB), L/R superior longitudinal fasciculus-parietal bundle (SLFp), L/R superior

Table 1
Demographics of the cohorts.

Group	Age	GenderM/F	Total FC	Digit span forward	Digit span backwards	HVLT delay	Stroop color	Symbol digit	Verbal fluency phonemic
Control	54.7 ± 8.8	14/23	13	11.5 ± 2.2	7.8 ± 2.9	29.5 ± 4.3	44.8 ± 10.7	52.5 ± 10.3	45.4 ± 13.5
PreHD	48.1 ± 11.5	13/18	12.04 ± 1.1	10.9 ± 1.9	7.7 ± 2.9	9.1 ± 2.7	69.6 ± 18.2	47.0 ± 12.6	46.4 ± 13.7
PHD$_{far}$	45.0 ± 9.8	5/5	12.1 ± 0.8	10.8 ± 1.5	8.3 ± 2.6	9.9 ± 2.3	75.6 ± 20.2	50.8 ± 13.9	47.2 ± 10.5
PHD$_{near}$	49.6 ± 12.2	8/13	12.0 ± 1.3	11.0 ± 2.4	7.2 ± 3.3	8.7 ± 2.8	66.4 ± 16.7	45.0 ± 11.9	45.9 ± 15.5
HD	55.2 ± 11.5	14/24	8.4 ± 2.6	9.3 ± 2.3	5.07 ± 1.98	5.3 ± 3.2	47.6 ± 19.6	27.9 ± 12.1	27.5 ± 15.7

Continuous variables are summarized using mean and stand deviation; categorical variables (i.e. gender) are listed as counts.

longitudinal fasciculus-temporal bundle (SLFt), for a total of 18 tracts.

2.2.4. Statistical analyses

Analysis of variance was used to compare age, education. The mean diffusion measures of control, PHD, and HD individuals were compared for each tract using Hotelling's T2 to compare pairs of groups. When there were significant differences (p < 0.05), post-hoc analyses were also performed. Spearman correlation coefficients were calculated to quantify the monotonic relationships between neuropsychological tests or cortical thinning and diffusivity measures. Due to the relatively small percentage of missing data, all calculations were performed using those subjects with available data. For each group (control, PHD (combined near- and far-PHD), and HD) unadjusted p-values were calculated that evaluated the null hypothesis that these measures were unrelated (i.e. $\rho = 0$). The false discovery rate adjusted p-values were also computed to account for multiple comparisons (Benjamini and Hochberg, 1995) and those that met a 0.1 threshold were highlighted (Genovese et al., 2002).

We accounted for the potential confound of head motion (Yendiki et al., 2014) by computing the average frame-by-frame translation and rotation over each subject's diffusion scan. We compared these motion measures between groups using one-way ANOVA, and we also used the two-sample Hotelling's T2 test for bivariate comparisons of translation and rotation between pairs of groups. We found no significant difference in motion measures amongst groups.

3. Results

3.1. Group differences in WM tract microstructural properties

Diffusion parameters (FA, AD, and RD) were extracted for each of the reconstructed pathways and the mean values for each calculated. For every combination of tract and location, the 3D mean vector and 3 × 3 covariance matrix for FA, AD, and RD were calculated. The boxplot, Fig. 1, demonstrates the tracts demonstrating significant differences in diffusion measures amongst the groups.

In early HD patients, the most significant decreases in FA versus controls were present in the FM, R/L CCG, L CST, R/L SLFp, and R/L SLFt. There were significant increases in RD in all tracts, with the exception of the R CAB, the R/L CST, and the L UNC, where trends were present. There were also significant increases in AD measures in all tracts with the exception of the R/L CAB, R/L CCG, and L SLFp. In PHD$_{near}$ subjects, the most significant decreases in FA were present in the R/L CCG, R ILF, L SLFp and R/L SLFt. Significant increases in RD were present in several tracts including R ATR, L CCG (with a trend on the R), L ILF, L SLFp and L SLFt; there were no significant differences in AD in any tract in these subjects. There were no significant differences in any diffusion measure in PHD$_{far}$ subjects.

3.2. Associations between cognitive measures and diffusion measures

We hypothesized that impaired performance on the HVLT would be associated with increases in RD in the CCG, a tract associated with limbic areas, as well as with the ATR, SLF (Madhavan et al., 2014) and ILF, tracts which have also been associated with cognitive dysfunction

in several other neurological disorders (Chanraud et al., 2010). We evaluated changes in RD of the forceps minor with tasks associated with attention. Finally, we evaluated changes in RD in the SLF and Forceps major and performance on the Stroop color and Symbol Digit, tasks which assess both attention, task switching, associative learning, and visuospatial processing. We found significant associations between RD (and not AD) with impaired performance on cognitive assessments, as summarized in Table 2, which also provides both the unadjusted and adjusted p-values.

3.3. Associations between regional cortical thickness and diffusion parameters

Significant associations were found in HD subjects (but not in controls or in Pre-HD subjects) between regional cortical thickness measures and AD, as summarized in Table 2 and illustrated in Fig. 2.

Correlations are summarized in Table 2 and shown in Fig. 2.

4. Discussion

White matter degeneration has been increasingly recognized as an early and important event in Huntington's disease. We evaluated changes in the microstructural integrity of large fiber bundles in HD and found regionally and temporally distinct changes, with the earliest changes in RD in PHD$_{near}$ subjects in whom RD was increased in several tracts, namely the CCG, ATR, SLF and ILF. In early symptomatic HD patients, there were additional increases in RD in the LCAB, UNC, Fmajor and Fminor. We did not find any significant changes in PHDfar. Together, these findings suggest that degeneration of myelin integrity may not only be early indicator of transition from health to disease, but may also represent a progressive process (Bartzokis et al., 2007). These findings are consistent with recent reports of thinner myelin sheaths, reduced expression of myelin-related genes, and aberrant ganglioside metabolism, which have been reported prior to neuronal loss in HD transgenic mice (Di Pardo et al., 2016; Teo et al., 2016) and support the importance of investigating the potential role of impaired oligodendrocytes in HD (Huang et al., 2015).

We also evaluated the relationship between increased RD and impaired performance, given the importance of myelination in synaptic function, signal transduction, and cognitive function (Fields, 2008). As hypothesized, we found associations between increases in RD and impaired performance on several neuropsychological tests in domains that have been well established as impaired in HD (Papoutsi et al., 2014). Increases in RD in the CCG were associated with impaired performance on the HVLT. The CCG is a supra-callosal fiber bundle positioned laterally and ventrally to the cingulate cortex that contains three principal fiber components: one from the thalamus, one from the cingulate gyrus and a third from association cortices (namely frontal, parietal and inferior temporal areas). An important function of this bundle is related to the communication between components of the limbic system (Mufson and Pandya, 1984) as well as with the execution of top-down and bottom-up attentional signals (Bonnelle et al., 2012). Disconnection of this fiber bundle has been associated with post-traumatic amnesia (De Simoni et al., 2016), with attention-deficit hyperactivity (Kabukcu Basay et al., 2016) and with Alzheimer's disease (Lee et al., 2015). We
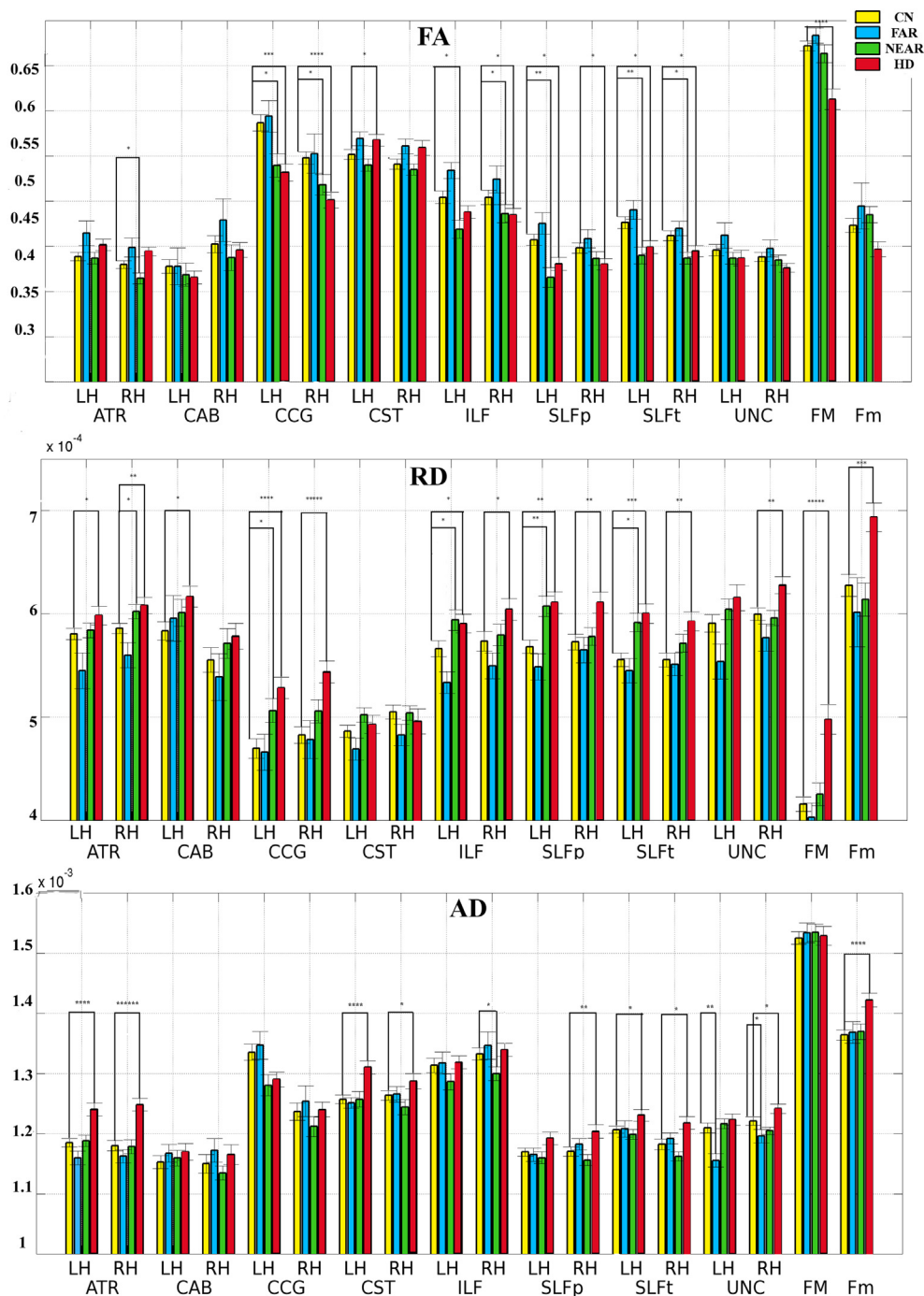
Fig. 1. Group comparisons of FA, MD, RD and AD between controls, PHD and HD participants. Error bars were constructed using 1 standard error from the mean. LH = left; RH = right; ATR = anterior thalamic radiations; CAG = cingulum-angular bundle; CCG = cingulum-cingulate gyrus bundle; CST = corticospinal tract; ILF = inferior longitudinal fasciculus; SLFp = superior longitudinal fasciculus-parietal endings; SLFt = superior longitudinal fasciculus temporal endings; UNC = uncinate fasciculus; FMAJOR = corpus callous-forceps major; FMINOR = corpus callosum-forceps minor.

also found an association between increases in RD in the ILF and impaired performance on the Symbol Digit. The ILF, a late myelinating fiber tract, is a ventral associative bundle connecting the temporal and occipital lobes. It plays an important role in visual object and face recognition (Unger et al., 2016) and has been implicated in disorders of visual perception, including in HD (Wolf et al., 2014; Nasr and Rosas, 2016). We found an association between impaired performance on the HVLT and increases in RD of the ATR. The ATR consists of fibers connecting medio-dorsal thalamic nuclei with frontal and anterior cingulate cortex. Disruption of the ATR has been found to impact memory encoding and executive functioning (Mamah et al., 2010), suggesting

that WM degeneration could predict cognitive deficits, such as these. Our findings are consistent with those reported by other groups (Dumas et al., 2012, Matsui et al., 2014), and suggest that disruption of the ATR may play a role in early executive dysfunction in HD more broadly. We also found an association between increased RD in the SLF and performance on the HVLT, Stroop and Symbol digit. The SLF is a bidirectional link between regions in frontal and parietal cortices (Makris et al., 2005) and subserves many complex tasks including regulating motor behavior (Cipolloni and Pandya, 1999), attention (Frye et al., 2010), working memory (Karlsgodt et al., 2008) and visual spatial functions (Hoeft et al., 2007). Finally, we found a relationship total

Table 2
Spearman's correlation between cognitive scores and radial diffusivity.

Neuropsychological scores		Tract		Group	Spearman's correlation, ρ	Unadjusted p-value ([a])
Total motor skills		CST	Right	Pre-HD	0.52	0.006[a]
Digit span	Forward	FMinor		HD	−0.34	0.051
HVLT delay		ATR	Left	Pre-HD	−0.40	0.028
		CCG	Left		−0.41	0.023
		SLFp	Left		−0.40	0.026 (0.030)
			Right		−0.49	0.006[a]
		ILF	Left		−0.53	0.003[a]
Stroop	Color	FMajor		HD	−0.59	< 0.001[a]
		SLFp	Left	Pre-HD	−0.45	0.012
			Right		−0.46	0.010
Symbol digit		FMajor		HD	−0.66	< 0.001[a]
		ILF	Left	Pre-HD	−0.43	0.017
			Right	HD	−0.47	0.006[a]
		SLFp	Left	Pre-HD	−0.38	0.036
			Right		−0.42	0.020
			Left	HD	−0.34	0.053
			Right		−0.52	0.002[a]

[a] Significant using false discovery rate adjusted threshold.
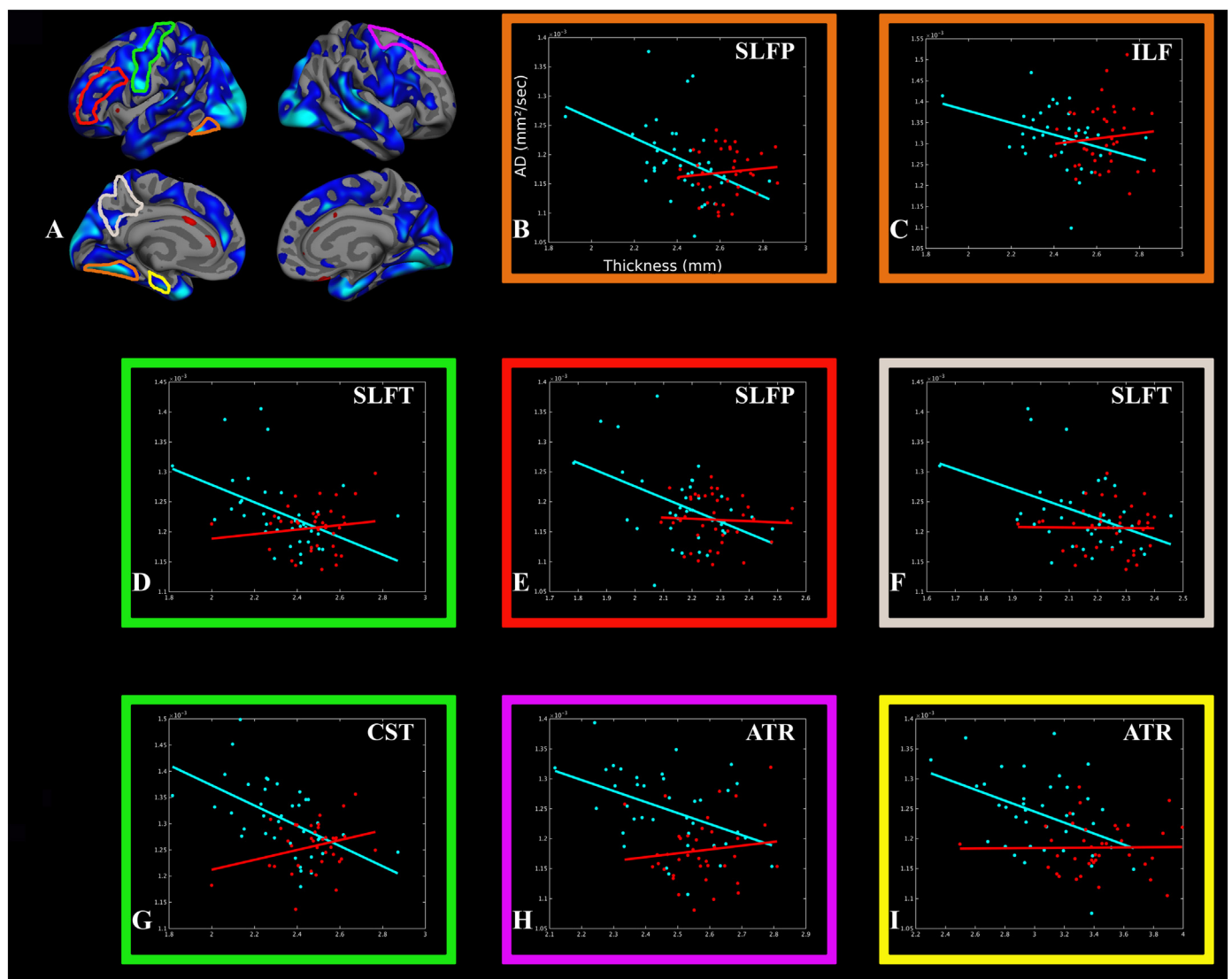
Fig. 2. Associations between regional cortical thickness and axial diffusivity. There were significant inverse correlations between AD and the thickness of associated cortical regions in HD (turquoise) but not in controls (red). The correlation plots are highlighted in the same color reflecting the cortical region associated with the respective tract. The x-axis corresponds to AD; the y-axis corresponds to cortical thickness. (For interpretation of the references to color in this figure legend, the reader is referred to the web version of this article.)

Table 3
Spearman's correlation between cortical thickness and axial diffusivity in HD subjects.

Cortical region	Tract		Spearman's correlation, ρ	Unadjusted p-value[a]
Entorhinal cortex	ATR	Left	−0.40	0.013
Fusiform	SLFp	Left	−0.53	0.001[a]
Parahippocampal	UNC	Left	−0.42	0.009
Precentral	ATR	Right	−0.45	0.005
	CST	Left	−0.0.59	< 0.001[a]
	SLFp	Left	−0.50	0.004
Rostral middle frontal	SLFt	Left	−0.41	0.010
Superior frontal	ATR	Right	−0.42	0.010
Superior temporal	SLFt	Left	−0.41	0.011
Supramarginal	SLFt	Left	−0.49	0.002[a]
Thalamus	ATR	Right	−0.56	< 0.001[a]

[a] Significant using false discovery rate adjusted p-value.

motor scores and the CST, as would be expected (Macdonald et al., 1997). Together, these findings suggest that alterations in the integrity of myelin may also play an important role in explaining early neuronal dysfunction (Koch et al., 2011), or altered neuronal circuitry (Ciarmiello et al., 2006) reflected as "soft" clinical signs during the HD prodrome.

We found significant increases in AD, which likely represents axonal loss attributable to Wallerian degeneration (Li et al., 2001; Song et al., 2003; Gatto et al., 2015) or possibly a consequence of oligodendrocyte dysfunction and its effect on axonal integrity and structure (Huang et al., 2015), in early symptomatic HD subjects in the ATR, CST, ILF, SLF, UNC and Fminor. Increases in AD were associated with regional atrophy (Rosas et al., 2008a) (Table 3). Higher AD of the CST was associated with greater thinning of the precentral cortex; higher AD in the ATR was associated with greater thalamic atrophy; higher AD in the SLF was associated with greater thinning of the supramarginal gyrus and fusiform cortex. These findings are consistent with increased accumulation of intra-nuclear and neuropil aggregates of N-terminal mutant huntingtin in dystrophic cortico-striatal axons in HD (DiFiglia et al., 1997; Sapp et al., 1999) and previous post-mortem studies that demonstrated reduced numbers of pyramidal neurons and their axonal connections (Cudkowicz and Kowall, 1990).

In summary, we show early and selective changes in the microstructural integrity of white matter in HD, associated with early deficits in myelin followed by axonal pathology, that are closely correlated with clinical symptoms and with cortical degeneration, and which suggest that oligodendroctyes might present a novel and important therapeutic target for HD.

Acknowledgments

Funding

Declaration of interest

Conflicts of interest for any author: None.

References

Agosta, F., Pievani, M., Sala, S., Geroldi, C., Galluzzi, S., Frisoni, G.B., et al., 2011. White matter damage in Alzheimer disease and its relationship to gray matter atrophy. Radiology 258 (3), 853–863.

Barkovich, A.J., Baranski, K., Vigneron, D., Partridge, J.C., Hallam, D.K., Hajnal, B.L., et al., 1999. Proton MR spectroscopy for the evaluation of brain injury in asphyxiated, term neonates. AJNR Am. J. Neuroradiol. 20 (8), 1399–1405.

Bartzokis, G., Lu, P.H., Tishler, T.A., Fong, S.M., Oluwadara, B., Finn, J.P., et al., 2007. Myelin breakdown and iron changes in Huntington's disease: pathogenesis and treatment implications. Neurochem. Res. 32 (10), 1655–1664.

Basser, P.J., Pierpaoli, C., 1996. Microstructural and physiological features of tissues elucidated by quantitative-diffusion-tensor MRI. J. Magn. Reson. Ser. B 111 (3), 209–219.

Benjamini, Y., Hochberg, Y., 1995. Controlling the false discovery rate: a practival and powerful approach to multiple testing. J. R. Stat. Soc. 57 (Series B), 289–300.

Bohanna, I., Georgiou-Karistianis, N., Sritharan, A., Asadi, H., Johnston, L., Churchyard, A., et al., 2011. Diffusion tensor imaging in Huntington's disease reveals distinct patterns of white matter degeneration associated with motor and cognitive deficits. Brain Imaging Behav. 5 (3), 171–180.

Bonnelle, V., Ham, T.E., Leech, R., Kinnunen, K.M., Mehta, M.A., Greenwood, R.J., et al., 2012. Salience network integrity predicts default mode network function after traumatic brain injury. Proc. Natl. Acad. Sci. U. S. A. 109 (12), 4690–4695.

Chanraud, S., Zahr, N., Sullivan, E.V., Pfefferbaum, A., 2010. MR diffusion tensor imaging: a window into white matter integrity of the working brain. Neuropsychol. Rev. 20 (2), 209–225.

Ciarmiello, A., Cannella, M., Lastoria, S., Simonelli, M., Frati, L., Rubinsztein, D.C., et al., 2006. Brain white-matter volume loss and glucose hypometabolism precede the clinical symptoms of Huntington's disease. J. Nucl. Med. 47 (2), 215–222.

Cipolloni, P.B., Pandya, D.N., 1999. Cortical connections of the frontoparietal opercular areas in the rhesus monkey. J. Comp. Neurol. 403 (4), 431–458.

Cudkowicz, M., Kowall, N.W., 1990. Degeneration of pyramidal projection neurons in Huntington's disease cortex. Ann. Neurol. 27 (2), 200–204.

De Simoni, S., Grover, P.J., Jenkins, P.O., Honeyfield, L., Quest, R.A., Ross, E., et al., 2016. Disconnection between the default mode network and medial temporal lobes in post-traumatic amnesia. Brain 139 (Pt 12), 3137–3150.

Delmaire, C., Dumas, E.M., Sharman, M.A., van den Bogaard, S.J., Valabregue, R., Jauffret, C., et al., 2013. The structural correlates of functional deficits in early Huntington's disease. Hum. Brain Mapp. 34 (9), 2141–2153.

Di Pardo, A., Amico, E., Maglione, V., 2016. Impaired levels of gangliosides in the corpus callosum of Huntington disease animal models. Front. Neurosci. 10, 457.

DiFiglia, M., Sapp, E., Chase, K.O., Davies, S.W., Bates, G.P., Vonsattel, J.P., et al., 1997. Aggregation of huntingtin in neuronal intranuclear inclusions and dystrophic neurites in brain. Science 277 (5334), 1990–1993.

Dumas, E.M., van den Bogaard, S.J., Ruber, M.E., Reilman, R.R., Stout, J.C., Craufurd, D., et al., 2012. Early changes in white matter pathways of the sensorimotor cortex in premanifest Huntington's disease. Hum. Brain Mapp. 33 (1), 203–212.

Fields, R.D., 2008. White matter in learning, cognition and psychiatric disorders. Trends Neurosci. 31 (7), 361–370.

Frye, R.E., Hasan, K., Malmberg, B., Desouza, L., Swank, P., Smith, K., et al., 2010. Superior longitudinal fasciculus and cognitive dysfunction in adolescents born pre-term and at term. Dev. Med. Child Neurol. 52 (8), 760–766.

Gatto, R.G., Chu, Y., Ye, A.Q., Price, S.D., Tavassoli, E., Buenaventura, A., et al., 2015. Analysis of YFP(J16)-R6/2 reporter mice and postmortem brains reveals early pathology and increased vulnerability of callosal axons in Huntington's disease. Hum. Mol. Genet. 24 (18), 5285–5298.

Genovese, C.R., Lazar, N.A., Nichols, T., 2002. Thresholding of statistical maps in functional neuroimaging using the false discovery rate. NeuroImage 15 (4), 870–878.

Greve, D.N., Fischl, B., 2009. Accurate and robust brain image alignment using boundary-based registration. NeuroImage 48 (1), 63–72.

Hoeft, F., Barnea-Goraly, N., Haas, B.W., Golarai, G., Ng, D., Mills, D., et al., 2007. More is not always better: increased fractional anisotropy of superior longitudinal fasciculus associated with poor visuospatial abilities in Williams syndrome. J. Neurosci. 27 (44), 11960–11965.

Huang, B., Wei, W., Wang, G., Gaertig, M.A., Feng, Y., Wang, W., et al., 2015. Mutant huntingtin downregulates myelin regulatory factor-mediated myelin gene expression and affects mature oligodendrocytes. Neuron 85 (6), 1212–1226.

Ishibashi, T., Dakin, K.A., Stevens, B., Lee, P.R., Kozlov, S.V., Stewart, C.L., et al., 2006. Astrocytes promote myelination in response to electrical impulses. Neuron 49 (6), 823–832.

Kabukcu Basay, B., Buber, A., Basay, O., Alacam, H., Ozturk, O., Suren, S., et al., 2016. White matter alterations related to attention-deficit hyperactivity disorder and COMT val(158)met polymorphism: children with valine homozygote attention-deficit hyperactivity disorder have altered white matter connectivity in the right cingulum (cingulate gyrus). Neuropsychiatr. Dis. Treat. 12, 969–981.

Karlsgodt, K.H., van Erp, T.G., Poldrack, R.A., Bearden, C.E., Nuechterlein, K.H., Cannon, T.D., 2008. Diffusion tensor imaging of the superior longitudinal fasciculus and working memory in recent-onset schizophrenia. Biol. Psychiatry 63 (5), 512–518.

Koch, K., Wagner, G., Schachtzabel, C., Schultz, C.C., Gullmar, D., Reichenbach, J.R., et al., 2011. Neural activation and radial diffusivity in schizophrenia: combined fMRI and diffusion tensor imaging study. Br. J. Psychiatry 198 (3), 223–229.

Langbehn, D.R., Hayden, M.R., Paulsen, J.S., 2010. CAG-repeat length and the age of onset in Huntington disease (HD): a review and validation study of statistical approaches. Am. J. Med. Genet. B Neuropsychiatr. Genet. 153B (2), 397–408.

Lee, S.H., Coutu, J.P., Wilkens, P., Yendiki, A., Rosas, H.D., Salat, D.H., et al., 2015. Tract-

based analysis of white matter degeneration in Alzheimer's disease. Neuroscience 301, 79–89.

Li, H., Li, S.H., Yu, Z.X., Shelbourne, P., Li, X.J., 2001. Huntingtin aggregate-associated axonal degeneration is an early pathological event in Huntington's disease mice. J. Neurosci. 21 (21), 8473–8481.

Macdonald, V., Halliday, G.M., Trent, R.J., McCusker, E.A., 1997. Significant loss of pyramidal neurons in the angular gyrus of patients with Huntington's disease. Neuropathol. Appl. Neurobiol. 23 (6), 492–495.

Madhavan, K.M., McQueeny, T., Howe, S.R., Shear, P., Szaflarski, J., 2014. Superior longitudinal fasciculus and language functioning in healthy aging. Brain Res. 1562, 11–22.

Makris, N., Kennedy, D.N., McInerney, S., Sorensen, A.G., Wang, R., Caviness Jr., V.S., et al., 2005. Segmentation of subcomponents within the superior longitudinal fascicle in humans: a quantitative, in vivo, DT-MRI study. Cereb. Cortex 15 (6), 854–869.

Mamah, D., Conturo, T.E., Harms, M.P., Akbudak, E., Wang, L., McMichael, A.R., et al., 2010. Anterior thalamic radiation integrity in schizophrenia: a diffusion-tensor imaging study. Psychiatry Res. 183 (2), 144–150.

Matsui, J.T., Vaidya, J.G., Johnson, H.J., Magnotta, V.A., Long, J.D., Mills, J.A., et al., 2014. Diffusion weighted imaging of prefrontal cortex in prodromal Huntington's disease. Hum. Brain Mapp. 35 (4), 1562–1573.

Mufson, E.J., Pandya, D.N., 1984. Some observations on the course and composition of the cingulum bundle in the rhesus monkey. J. Comp. Neurol. 225 (1), 31–43.

Nasr, S., Rosas, H.D., 2016. Impact of visual Corticostriatal loop disruption on neural processing within the parahippocampal place area. J. Neurosci. 36 (40), 10456–10471.

Papoutsi, M., Labuschagne, I., Tabrizi, S.J., Stout, J.C., 2014. The cognitive burden in Huntington's disease: pathology, phenotype, and mechanisms of compensation. Mov. Disord. 29 (5), 673–683.

Paulsen, J.S., Miller, A.C., Hayes, T., Shaw, E., 2017. Cognitive and behavioral changes in Huntington disease before diagnosis. Handb. Clin. Neurol. 144, 69–91.

Pierpaoli, C., Barnett, A., Pajevic, S., Chen, R., Penix, L.R., Virta, A., et al., 2001. Water diffusion changes in Wallerian degeneration and their dependence on white matter architecture. NeuroImage 13 (6 Pt 1), 1174–1185.

Pievani, M., Agosta, F., Pagani, E., Canu, E., Sala, S., Absinta, M., et al., 2010. Assessment of white matter tract damage in mild cognitive impairment and Alzheimer's disease. Hum. Brain Mapp. 31 (12), 1862–1875.

Poudel, G.R., Stout, J.C., Dominguez, D.J., Salmon, L., Churchyard, A., Chua, P., et al., 2014. White matter connectivity reflects clinical and cognitive status in Huntington's disease. Neurobiol. Dis. 65, 180–187.

Rosas, H.D., Tuch, D.S., Hevelone, N.D., Zaleta, A.K., Vangel, M., Hersch, S.M., et al., 2006. Diffusion tensor imaging in presymptomatic and early Huntington's disease: selective white matter pathology and its relationship to clinical measures. Mov. Disord. 21 (9), 1317–1325.

Rosas, H.D., Salat, D.H., Lee, S.Y., Zaleta, A.K., Hevelone, N., Hersch, S.M., 2008a. Complexity and heterogeneity: what drives the ever-changing brain in Huntington's disease? Ann. N. Y. Acad. Sci. 1147, 196–205.

Rosas, H.D., Salat, D.H., Lee, S.Y., Zaleta, A.K., Pappu, V., Fischl, B., et al., 2008b. Cerebral cortex and the clinical expression of Huntington's disease: complexity and heterogeneity. Brain 131 (Pt 4), 1057–1068.

Rosas, H.D., Lee, S.Y., Bender, A.C., Zaleta, A.K., Vangel, M., Yu, P., et al., 2010. Altered white matter microstructure in the corpus callosum in Huntington's disease: implications for cortical "disconnection". NeuroImage 49 (4), 2995–3004.

Rosas, H.D., Reuter, M., Doros, G., Lee, S.Y., Triggs, T., Malarick, K., et al., 2011. A tale of two factors: what determines the rate of progression in Huntington's disease? A longitudinal MRI study. Mov. Disord. 26 (9), 1691–1697.

Sapp, E., Penney, J., Young, A., Aronin, N., Vonsattel, J.P., DiFiglia, M., 1999. Axonal transport of N-terminal huntingtin suggests early pathology of corticostriatal projections in Huntington disease. J. Neuropathol. Exp. Neurol. 58 (2), 165–173.

Song, S.K., Sun, S.W., Ju, W.K., Lin, S.J., Cross, A.H., Neufeld, A.H., 2003. Diffusion tensor imaging detects and differentiates axon and myelin degeneration in mouse optic nerve after retinal ischemia. NeuroImage 20 (3), 1714–1722.

Teo, R.T., Hong, X., Yu-Taeger, L., Huang, Y., Tan, L.J., Xie, Y., et al., 2016. Structural and molecular myelination deficits occur prior to neuronal loss in the YAC128 and BACHD models of Huntington disease. Hum. Mol. Genet. 25 (13), 2621–2632.

Unger, A., Alm, K.H., Collins, J.A., O'Leary, J.M., Olson, I.R., 2016. Variation in white matter connectivity predicts the ability to remember faces and discriminate their emotions. J. Int. Neuropsychol. Soc. 22 (2), 180–190.

Wolf, R.C., Sambataro, F., Vasic, N., Baldas, E.M., Ratheiser, I., Bernhard Landwehrmeyer, G., et al., 2014. Visual system integrity and cognition in early Huntington's disease. Eur. J. Neurosci. 40 (2), 2417–2426.

Yendiki, A., Panneck, P., Srinivasan, P., Stevens, A., Zollei, L., Augustinack, J., et al., 2011. Automated probabilistic reconstruction of white-matter pathways in health and disease using an atlas of the underlying anatomy. Front. Neuroinform. 5, 23.

Yendiki, A., Reuter, M., Wilkens, P., Rosas, H.D., Fischl, B., 2014. A probabilistic method for unbiased longitudinal tractography with application to Huntington's disease. Proc. Int. Soc. Magn. Reson. Med. 2014, 4530.

Yu, Z.X., Li, S.H., Evans, J., Pillarisetti, A., Li, H., Li, X.J., 2003. Mutant huntingtin causes context-dependent neurodegeneration in mice with Huntington's disease. J. Neurosci. 23 (6), 2193–2202.